Available online at www.sciencedirect.com
SCIENCE DIRECT®
PERGAMON
International Journal of Multiphase Flow 29 (2003) 841–854
International Journal of Multiphase Flow
www.elsevier.com/locate/ijmulflow

Analysis of wall shear stress in wet foam flows using the electrochemical method

P. Tisné *, F. Aloui, L. Doubliez

GEPEA UMR-CNRS 6144, Faculté des Sciences et des Techniques, Université de Nantes, 2, rue de la Houssinière, B.P. 92208, 44322 Nantes Cedex 3, France

Received 1 July 2002; received in revised form 19 February 2003

Abstract

In order to determine experimentally the wall shear stresses exerted on a wet foam which is flowing in a horizontal square duct, we examined here the use of a totally innovative method in foam flows: the electrochemical method. We showed that it was necessary to determine the film thickness when the latter is less than a certain critical thickness which is numerically estimated. We experimentally measured the film thickness by conductimetry and showed that the electrochemical signal fluctuations rightly reflected the shear stress fluctuations. We can conclude that the wall shear stress is more important between the bubbles than under the bubbles, like inside a capillary.

Keywords: Rheology; Horizontal square duct; Wet foam; Conductimetric method; Thin liquid film; Electrochemical method; Wall shear stress

1. Introduction

Aqueous foams have a number of industrial applications, which currently include fire extinguishing and oil refining. They are also prevalent in the food and chemical industries and in nuclear engineering.

Recent research in foams has centered on two main topics, which are often treated separately, but are in fact interdependent: stability (drainage and coarsening) and rheology (relative motion of bubble). We focus here on the study of wet foams flow behaviour through pipes, that is to say, wet foams rheology. As yet, there is no method to enable the prediction of pressure losses in the

* Corresponding author.
E-mail address: patrice.tisne@physique.univ-nantes.fr (P. Tisné).

0301-9322/03/$ - see front matter
doi:10.1016/S0301-9322(03)00038-7

pipe flow of foams, since foam exhibits many complex flow properties such as compressibility, shear thinning, elasticity, yield stress, and slippage at the pipe wall.

To make predictions of foam behaviour through pipes, some phenomena need to be better understood. The viscous bulk flow of foams and the apparent slip of foam are the two principal phenomena (Kraynick, 1988). This last phenomenon, the slip, is taken into account in many studies in order to characterize the fluid (Wenzel et al., 1970; Kroezen et al., 1988; Thondavadi and Lemlich, 1985; Calvert and Nezhati, 1986; Prud'homme and Khan, 1996).

On the macroscopic scale, Calvert (1990) and other authors such as Yoshimura and Prud'homme (1988) consider that the foam flow is dominated by the properties of a thin boundary region, which produce the slip effect. The bulk properties, which are used in conventional methods, are less important to overall flow behaviour. In particular, Calvert (1990) presents a model for predicting pressure losses and consequently the wall shear stress. He estimates the wall shear stress by a theory for plug flow. Near a solid surface, bubble migration leads to a liquid-rich layer, which gives the effect of slip between the foam and the wall. He expects the slip-layer thickness to be similar to the interbubble lamella thickness, which is related to the bubble size and the void fraction. This thickness is estimated to be of the order of ten of micrometers for typical foams. This small size, combined with the high value of the viscosity of the foam, means that a large proportion of the velocity variation in pipe flow occurs across the slip layer even in cases where the foam is shearing. The shear stress is virtually assumed constant across the slip layer and depends essentially on the film thickness by the relationship $\tau_0 = \eta_L V_g/\delta$ where τ_0 is the wall shear stress, η_L the viscosity of the liquid, V_g the bulk velocity and δ the slip layer thickness. Several authors such as Enzendorfer et al. (1994), Gardiner et al. (1999) use other similar relationships between the wall shear stress, the film thickness and the slip velocity. In fact, all these authors assume that in foam flows in duct, the wall liquid film is sheared.

In a parallel direction, other authors such as Ratulowski and Chang (1989), Harris et al. (1994) have theoretically analysed the wall shear stress in the slug flows in capillaries. This time, the study is on the microscopic scale, and the local mechanisms are proving to be dissimilar to the macroscopic scale mechanisms. According to them, the resistance to the plug flow comes mainly from the drag of the bubble. The drag is the force exerted by a capillary wall on the liquid film surrounding the bubble, and is evaluated by integration of the streamwise viscous shear stress over the wall. As the wetting fluid is dragged by the wall into the film, it experiences the largest shear stress just before entering the film. A similar mechanism at the back end of the film generates another peak in the shear stress. The thin film between the two caps is stagnant. The wall shear stress is not constant; the shear essentially occurs at the ends of the bubble.

In foams flow, an experimental study of the wall shear stress is proving interesting because it links the macroscopic and microscopic scales. In order to determine its value in the different points of a cross section, we examined here the use of electrochemical method (or polarographic method). It is regularly used in single-phase flow. It has been also adapted to liquid–gas flow but only for flows with few bubbles or with air slugs (Souhar, 1982; Lusseyran, 1990). In foam flows, it is a totally innovative method.

First, we theoretically analysed the effect of the wall film thickness on the mass transfer probe. This analysis permits to verify if the wall film is thick enough to use the theoretical results obtained for a semi-infinite medium. Film thickness measures are obtained by conductimetry in the same time as the electrochemical signals.

2. Theoretical analysis of the effect of the film thickness on the wall shear stress

We examined here the use of the electrochemical method to a wet foam flow in horizontal duct. Its fundamental principles are described by Reiss and Hanratty (1963), Cognet (1968), Lebouché (1968) and Souhar (1982).

This method of wall shear stress measurement remains valid in a two-phase flow, provided that the wall remains sufficiently wetted by a liquid film. In fact, the classical use of the electrochemical method assumes that the diffusion boundary layer must be thinner than the sheared film (Fig. 1).

The electrochemical system involved here is the reduction of ferricyanide ions on a platinum electrode (cathode). The method is based on the transfer of an active ion from the bulk of an electrolyte solution to the probe.

To study the film thickness effect on the concentration boundary layer near an electrochemical probe, we considered a two-dimensional flow on an horizontal plate. The general equation governing mass transfer is:

$$\frac{\partial c}{\partial t} + u\frac{\partial c}{\partial x} + v\frac{\partial c}{\partial y} = D\left(\frac{\partial^2 c}{\partial x^2} + \frac{\partial^2 c}{\partial y^2}\right) \tag{1}$$

where x is the direction of the mean flow, y the distance from the wall, u the velocity component in the x-direction, v the velocity component in the y-direction, c the concentration of the ferricyanide ion and D the molecular diffusion coefficient.

We suppose a steady shear flow. So, the velocity component u within the concentration boundary layer is characterised by:

$$u = S_0 y \quad \text{and} \quad v = 0 \tag{2}$$

where S_0 is the velocity gradient at the wall.

If we consider a steady flow over the probe, Eq. (1) becomes:

$$S_0 y\frac{\partial c}{\partial x} = D\left(\frac{\partial^2 c}{\partial x^2} + \frac{\partial^2 c}{\partial y^2}\right) \tag{3}$$

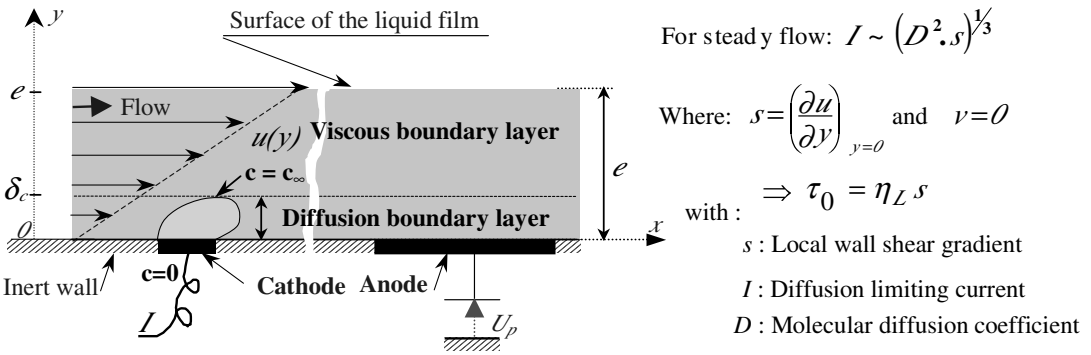

Fig. 1. Electrochemical method principle.

For a steady flow, the small electrode mounted flush with the insulating wall (Fig. 1) delivers a current I. This measured intensity increases with the applied voltage until the potential between the two electrodes is such that the current flowing in the circuit is controlled by the rate of diffusion of the reacting species to the surface of the working electrode. It then stabilises to a value named limiting current. The probe then behaves as a perfect mass sink. The average limiting current given by the Levêque formula (1928) is:

$$I = 0.807nFAc_\infty\left(\frac{D^2S_0}{l}\right)^{1/3} \tag{4}$$

where A is the electrode area, l the effective length of the electrode, F the Faraday constant (equal to 96500 Coulomb), c_∞ the bulk active ion concentration, n the number of electrons involved in the redox reaction.

For *Newtonian* liquid, the wall shear stress τ_0 is deduced from the velocity wall gradient S_0 by the relationship:

$$\tau_0 = \eta_L S_0 \tag{5}$$

where η_L represents the dynamic viscosity.

As the magnitude order of the diffusion boundary layer is given by:

$$\delta_C = \left(\frac{Dl}{S_0}\right)^{1/3} \tag{6}$$

we introduce the following dimensionless quantities:

$$C = \frac{c}{c_\infty}; \quad X = \frac{x}{l} \quad \text{and} \quad Y = \frac{y}{\delta_c}$$

Thus, Eq. (3) becomes:

$$Y\frac{\partial C}{\partial X} = \left(\frac{\delta_C}{l}\right)^2\frac{\partial^2 C}{\partial X^2} + \frac{\partial^2 C}{\partial Y^2} \tag{7}$$

Or, if the *Peclet* number Pe is defined by:

$$Pe = \left(\frac{S_0 l^2}{D}\right) \tag{8}$$

the equation governing the mass transfer (3) can be reduced to:

$$Y\frac{\partial C}{\partial X} = Pe^{-2/3}\frac{\partial^2 C}{\partial X^2} + \frac{\partial^2 C}{\partial Y^2} \tag{9}$$

In the case where the liquid film has a finished thickness e, the boundary conditions are shown on Fig. 2.

The convection diffusion equation (9) is numerically solved by using the finite difference approximation method for $10^{-4} \leqslant Pe \leqslant 10^8$. For these parameters, we varied the range of (e/δ_c) between 1 and 15 in order to determine from which value of (e/δ_c) we can have $C \approx 1$ at the surface of the liquid film. Thus, the film may be considered as a semi-infinite medium.

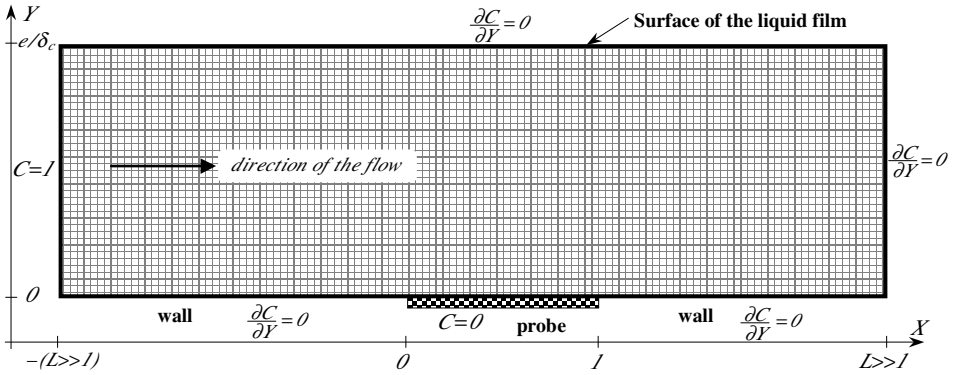

Fig. 2. Boundary conditions used for the numerical solution.

This numerical solution of the dimensionless concentration C leads to the determination of the mass flux, which is characterized by the average *Sherwood* number $\overline{Sh}$ on the probe surface. This number is defined as:

$$\overline{Sh} = \frac{I}{nFAc_\infty D} l \tag{10}$$

where the current I is:

$$I = nF \int\int_A D\left(\frac{\partial c}{\partial y}\right)_{y=0} \mathrm{d}A \tag{11}$$

Here, for the two dimensional flow:

$$\overline{Sh} = \frac{l}{\delta_C} \int_0^1 \left.\frac{\partial C}{\partial Y}\right|_{Y=0} \mathrm{d}X = Pe^{1/3} \int_0^1 \left.\frac{\partial C}{\partial Y}\right|_{Y=0} \mathrm{d}X \tag{12}$$

For the higher *Peclet* numbers, the streamwise diffusion becomes negligible. Therefore, for a semi-infinite medium, the calculated values of $\overline{Sh}$ are very close to the analytical solution given by Levêque (4) for a rectangular electrode:

$$\overline{Sh} = 0.807 Pe^{1/3} \tag{13}$$

For a circular electrode of diameter d and of the same area A, Reiss and Hanratty (1963) showed the length l may be replaced by $0.82d$ so that:

$$\overline{Sh}_{\mathrm{circ}} = \frac{I}{nFAc_\infty D} d = 0.862\left(\frac{d^2 S_0}{D}\right)^{1/3} \tag{14}$$

In Fig. 3, curves of $\overline{Sh}_{\mathrm{circ}}$ versus e are plotted for different values of the wall shear stress τ_0, for the conditions corresponding to our experiments: $\eta_{\mathrm{L}} = 1.1 \times 10^{-3}$ Pa s, $d = 0.25$ mm, $l = 0.82d$ and $D = 7.26 \times 10^{-10}$ m^2 s^{-1}.

These curves show that the maximum mass flux is reached when the film thickness exceeds a critical value e_c, which depends on S_0. So, this critical thickness value knowledge is very important

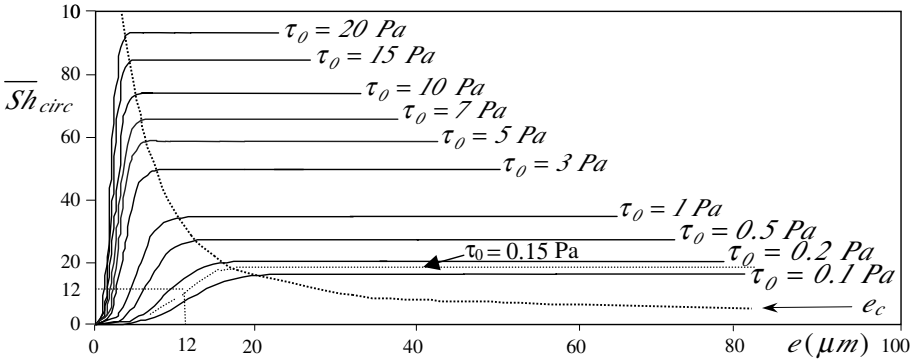

Fig. 3. $\overline{Sh}_{circ}$ profiles function of the liquid film thickness for different values of wall shear stress τ_0.

for the experimental application of the electrochemical method to the wet foam flows because the liquid film between the wall and the foam is very thin.

3. Experimental devices and measurement techniques

3.1. Experimental device

A schematic diagram of the principal experimental device is presented in Fig. 4. This device involves a recirculating liquid circuit regulated at 20.0 ± 0.5 °C and an open gas circuit (nitrogen)

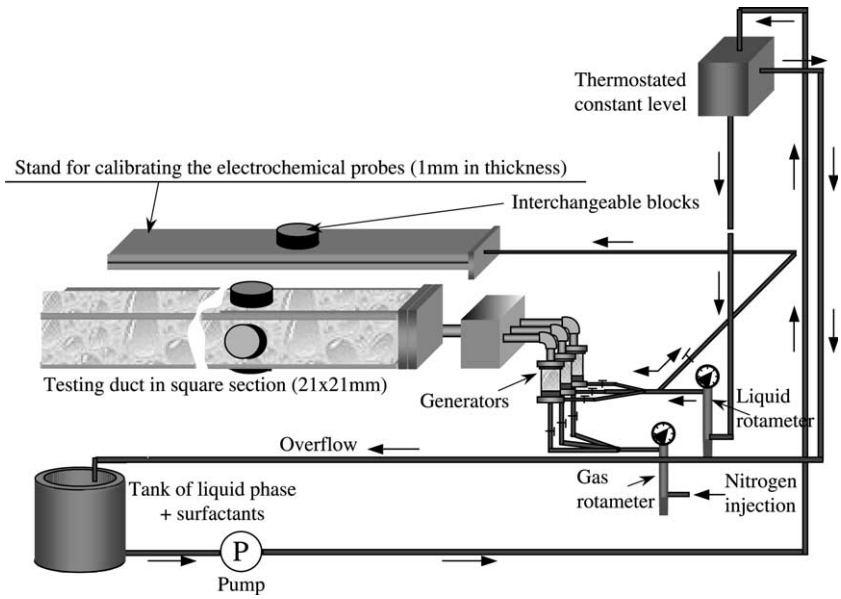

Fig. 4. Principal experimental device.

which supply the horizontal testing duct. This duct, in Plexiglass, is 2.5 m in length, and its cross section is square (21×21 mm^2). It's fixed on supports allowing to adjust to the horizontal position. Its outlet is opened to the atmosphere. The liquid and the nitrogen, at constant flow rates, feed three cylindrical containers (40 mm in internal diameter) using foam generators located at the stand inlet. These three foam generators are mounted in parallel. They allow to vary the flow rate. The foam is generated by nitrogen injection through a metallic sintered plate (about 2 μm in porosity).

In the duct, we may observe that the foam flows over a thin liquid layer (Blondin and Doubliez, 2002). This layer (about 1.5 mm) arises from the liquid carried away by the bubbles at the generators exit and is also fed by the foam drainage along the duct.

To measure the wall shear stress, we use the electrochemical method. Its application will be discussed below. Eleven small probes are flush mounted on each of three removable cylindrical insulating blocks and each of probes is polarized so as to have the diffusion limiting current. These blocks may be inserted at half-length of the duct on three sides: at the top, at the bottom, and at one lateral wall. For that, three holes are drilled in the duct so that the surfaces of the probes are flush with the wall.

The 11 platinum probes (0.25 mm in diameter) inserted in the blocks are aligned perpendicular to the flow and equally spaced 2 mm apart. Fig. 5a shows the probes positions. For their calibration, the supporting blocks are inserted to an auxiliary stand.

Each of the removable blocks used for the electrochemical method can be replaced by blocks fitted out for the thickness measurements by conductimetry. For this, we use two blocks, each one consisting of two probes. The choice of the probes (geometry and distance between the probes) depends on the liquid film thickness that we wish to measure. The farther the probes, the greater the film thickness that can be measured (Coney, 1973). A first block is used for the measure of the film thickness on the lateral wall and at the top. The probes are 0.25 mm in diameter (equivalent to a surface of 0.2 mm^2) and are spaced 40 μm apart (±2 μm). A second block is used for film thickness measurement at the bottom of the duct. The probes used are this time larger (surface about 40 mm^2) and spaced 6 mm apart.

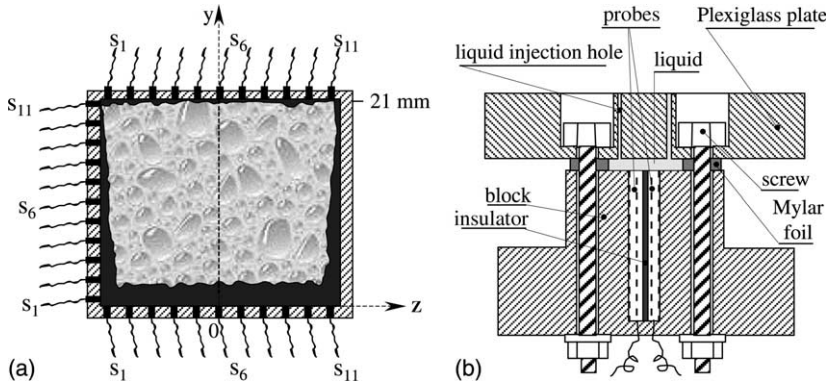

Fig. 5. (a) Electrochemical probes positions. (b) Calibration device of conductimetric probes.

3.2. Measurement techniques

3.2.1. Electrochemical method (calibration of the probes)

All the electrochemical probes are calibrated on an auxiliary circuit, which is presented on Fig. 4. This circuit principally consists in a rectangular horizontal duct (21×1 mm^2) 1 m in length. The wall shear stress is of the same order as the one estimated in the principal duct.

In the rectangular duct, the single-phase flow (liquid) is laminar. We measure the pressure drop ΔP and the current intensity I.

Varying the flow rate, we draw from each electrode its response curve giving the current I versus the wall shear stress τ_0. The τ_0 value is deduced from the pressure drop by $\tau_0 = D_H \cdot \Delta P/(4L)$, where L is the length between the two pressure taps and D_H is the hydraulic diameter of the rectangular duct. From the relationship (4), we determine the effective diameter d of each electrode and the corresponding Sherwood value $\overline{Sh}_{circ} = I \cdot d/(nFAc_\infty D)$ associated to the wall shear stress $S_0 = \tau_0/\eta_L$.

To ascertain that the calibration of all the electrochemical probes has been accurately accomplished in the auxiliary duct, we compared these calibration results with those obtained by the Cotrell method. This technique is based on the study of the transient response of the probes to a voltage step from 0 to the diffusional plateau potential; it is described in details by Sobolik et al. (1996). Before the stationary regime is obtained, the current decreases following the Cotrell asymptote. During this period of time, the evolution of the electrical intensity as a function of $1/\sqrt{t}$ is linear. The slope permits to deduce the active electrode area and therefore the value of the effective diameter d of the probe. This value of d by this technique is about the same as the one deduced from the pressure drop, $\pm 1\%$. Therefore, we have a good agreement between the two calibration techniques.

3.2.2. Conductimetric method

The measurement of wall film thickness is proving primordial to verify if this thickness remains sufficient to apply the electrochemical method. For this, we used the conductimetric method. In fact, we measure the conductance of a film portion between two electrodes flush mounted to the wall. The probes are supplied with a conductimeter, which provides an alternative sine wave signal voltage. The frequency is 50 kHz to avoid polarisation phenomena.

The two blocks used for the thickness measurement are removable in order to calibrate the probes in a secondary circuit. The calibration device (Fig. 5b) is made of a Plexiglass plate to which we screwed the block. The distance h between the plate and the block can be adjusted by means of calibrated Mylar foils. The foaming solution fills the space between the plate and the block. The experimental relationship giving the current as a function of h is established for each pair of probes. For the first block used to measure the thickness on the lateral wall and at the top, the response is linear in so far as the thickness is less than 100 μm. For the second block (used to measure the thickness at the bottom), the response is linear in so far as the thickness is less than 3 mm. When the probes are used with foam, the wall wetting liquid is surrounded by bubbles. Consequently, its thickness is not uniform and moreover the foam is not an insulating medium. To estimate the discrepancy between a measurement made with a film of uniform thickness and an irregular wetting film, we used an analogous arrangement with an electrical conducting paper (Teledeltos). The bubbles are simulated by holes in the paper and the two electrodes by two strips

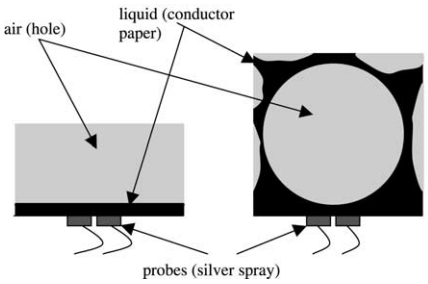

Fig. 6. Electrical analogy.

of silver spray (Fig. 6). When the bubble diameters are twice the electrode length, the current is just altered by 3%. So, for the foam used in our experiments, we consider that the local film thickness may be deduced from the current value with a sufficient accuracy.

The tightening of the two blocks leads to a total measurement uncertainty of about 12%.

3.3. Foaming solution

The foaming agents Amonyl and Symulsol (supplied by SEPPIC) are chosen to support the electrolyte, which is used for the electrochemical method. The liquid was composed of distilled water with:

- 0.1% by weight of Amonyl (an anionic surfactant),
- 0.1% by weight of Symulsol (a non ionic surfactant),
- the oxido–redox couple: ferricyanide ($c = 10$ mol/m^3), ferrocyanide ($c = 30$ mol/m^3),
- the supporting electrolyte used for neutralizing the active ions migration induced by the potential field created between the anode and the cathode: potassium sulphate ($c = 350$ mol/m^3).

4. Results and discussions

The runs presented here are effected with a gas flow rate of 6.1 cm^3/s and a liquid flow rate of 2.6 cm^3/s corresponding to a gas volumic fraction of 70% and a mean velocity of 2 cm/s. The bubble size is about 1 mm in diameter. With these conditions, the foam flows as a plug and the liquid layer under the foam is 1.5 mm thick. The pressure gradient is 600 Pa/m in the test section.

4.1. Wall film thickness

The signals given by the conductance probes show great fluctuations at the lateral wall and at the top (Fig. 7). We have simultaneously recorded the probes current and images of the bubbles coming into contact with the probes. It can be verified that the fluctuations are well correlated with the bubbles passing over the probe.

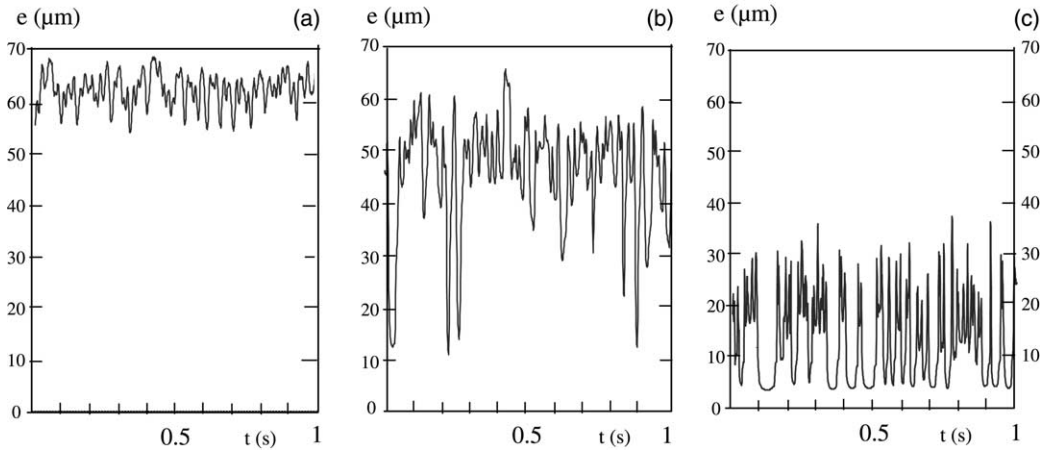

Fig. 7. Wall film thickness evolution for $\overline{V} = 2$ cm/s: (a) at 2.5 mm from the bottom of the duct on the lateral wall; (b) at the middle of the lateral wall; (c) at the top of the duct.

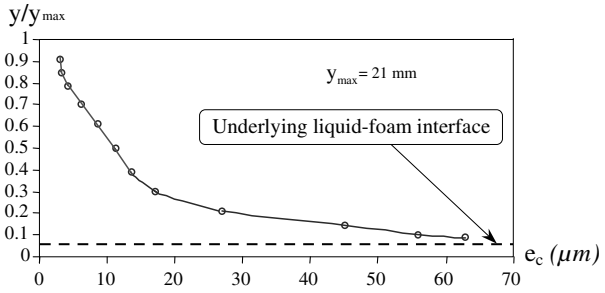

Fig. 8. Minimal thickness evolution on the lateral wall for a plug flow and for a mean velocity of 2 cm/s.

At the top, the signals are similar, whatever the position of the probe, either in the middle or on the sides of the duct. The thickness varies from 5 μm straight above a bubble to 30 μm between the bubbles.

At the lateral wall, the minimal thickness (corresponding to the bubbles) increases from top to bottom. It is about 5 μm at the upper probe like at the top wall, and 65 μm just above the level of the underlying liquid film (Fig. 8). The thickening is due to the foam drainage.

4.2. Electrochemical signals

Typical signals of probes are shown on Fig. 9. The Sherwood temporal evolution is an indication of the wall shear stress fluctuations. We can observe that they are almost constant and identical from one probe to another at the bottom in the underlying liquid. However, in the presence of the foam, the measured currents fluctuate strongly. Fluctuation amplitudes increase with the altitude in the duct. At the top of the duct, these amplitudes are almost the same.

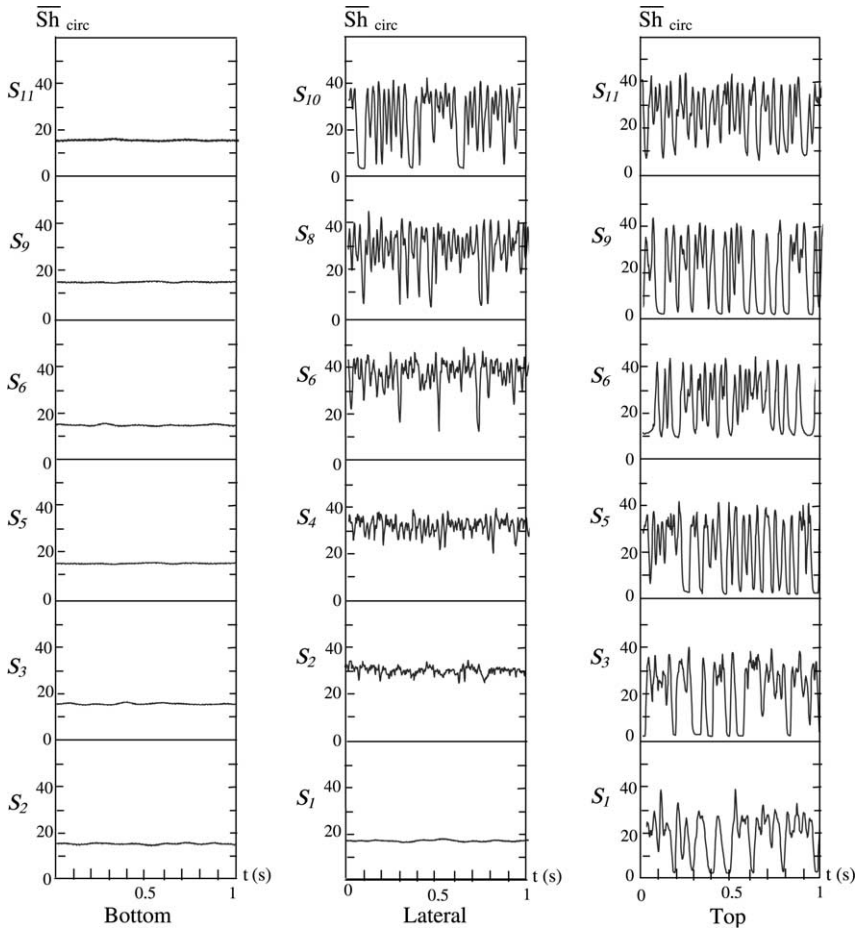

Fig. 9. Electrochemical temporal signals for a plug flow and for a mean velocity of 2 cm/s.

It should be observed that the Sherwood number and so the wall shear stress is always large enough that diffusion in the x-direction is not important.

In order to find the fluctuations origin, we monitored simultaneously video images of the wet foam flow and the electrochemical probe current. Fig. 10 shows the passage of the bubbles along the probe and the corresponding temporal electrochemical signal. For this run, the velocity of the foam is 0.8 cm/s and the visualisation is easier to make. We can then observe that the smaller values of the current coincide with the passage of bubbles distorted by the wall contact. The velocity under the bubbles is therefore lower than the velocity between the bubbles. We really think that the film under the bubbles is almost stagnant; the bubbles have a caterpillar motion as in a Hele–Shaw cell (Burgess and Foster, 1990). Moreover, it should be observed that our probes do not give the direction of the flow. But, the bubbles and liquid film flow is co-current. The double probes utility is not necessary. There is no counter current effect.

We are faced with the question as to whether the minima are due to a real decrease of the wall shear stress or due to an abatement of the current linked with the local thickness reduction.

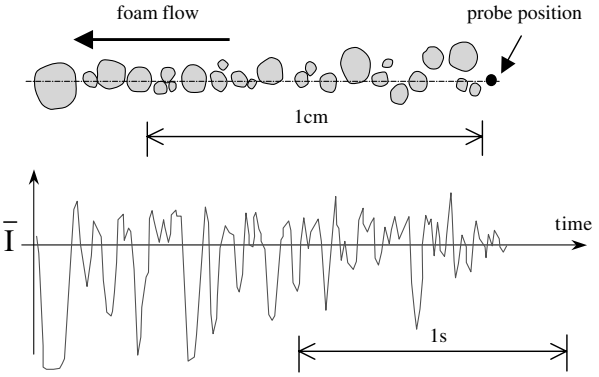

Fig. 10. Synchronisation of bubble passage with the electrochemical voltage signal for a mean velocity of 0.8 cm/s.

4.3. Discussions

If we consider the signal given by probe S_2 located at 2.5 mm from the bottom of the duct on the lateral wall (Fig. 9), the minima of the Sherwood number value is $Sh = 26$ and the measured minimal thickness is about 55 μm (Fig. 7a). The diffusion layer is less than the film thickness (Fig. 3) so that the shear stress is about 0.4 Pa, the critical thickness being about 12 μm.

At the middle of the lateral wall (probe S_6), the Sherwood number minimal value is about 12 (Fig. 9) and the minimal thickness (Fig. 7b) is about 12 μm. The shear stress deduced from Fig. 3 is 0.15 Pa. There is a noticeable abatement of the current. Between the bubbles, the Sherwood value is about 40 for the S_6 probe and therefore the wall shear stress is about 1 Pa. Then, the shear stress under the bubbles remains lower than the one between the bubbles whatever the probes location. There is a real decrease of the shear stress when a bubble crosses over a polarographic probe.

At the top of the duct, we can also conclude likewise. The minimal thickness is reduced to 5 μm (Fig. 7c), and the mean corresponding Sherwood number is 8. Then the uncertainty for the stress is higher but here also we may assess that the minima observed for the electrochemical signals correspond to the minima for the shear stress and that these minima coincide with the bubble passage over the probe.

Through all the signals, both on the lateral wall and at the top of the duct, we can conclude that the minima are rightly due to a real decrease of the wall shear stress. The smaller values of the current coincide with the passage of bubbles.

However, there can be a difficulty in deducing the effective shear stress from the measured current. It is linked to the non-linearity of frequency responses of the probe. This question has been studied for small amplitudes (Mitchell and Hanratty, 1966; Nakoryakov et al., 1986; Ambari et al., 1986; Deslouis et al., 1990), but for large amplitudes, like in the present case, studies are more limited (Mao and Hanratty, 1991; Funfschilling, 2001) and prove the interest of a numerical simulation of flows so as to establish the relationship between the current and the shear stress. The question of the frequency response remains still largely debated and we shall satisfy ourselves with a more qualitative than quantitative interpretation.

Nevertheless, we can already conclude from the signals that the wall shear stresses are lower in the films under the bubbles than in the intermediate zones between the bubbles. We find results

similar to those established theoretically for bubble flows inside capillaries (Ratulowski and Chang, 1989; Harris et al., 1994). According to Ratulowski and Chang (1989) and Harris et al. (1994), in a polygonal capillary the liquid flows by pushing the bubble (plug flow) and by by-passing the bubble through corner channels (corner flow). The resistance to the plug flow comes mainly from the drag of the bubble which is concentrated at two ends of a long bubble and not along the bubble.

5. Conclusion

The present investigation provides insight on the use of the electrochemical method. For a given probe diameter, when the film thickness is less than a critical value, the probe current is reduced.

We especially notice that the smaller wall shear stresses are in the films under the bubbles and not in the intermediate zones between the bubbles. The friction is especially concentrated at the two ends of the bubbles.

The use of this method simultaneously requires both the film thickness measurement and the acquisition of the electrochemical signal. Moreover, the frequency response of probes also remains an important question.

Once these conditions are satisfied, the momentum balance will be checked. Then, this will allow the deduction of the shear stress field throughout the whole section.

References

Ambari, A., Deslouis, C., Tribollet, B., 1986. Frequency response of the mass transfer rate in a modulated flow at electrochemical probes. Int. J. Heat Mass Transfer 29, 35–45.

Blondin, E., Doubliez, L., 2002. Particle imaging velocimetry of a wet aqueous foam with an underlying liquid film. Exp. Fluids 32, 294–301.

Burgess, D., Foster, M.R., 1990. Analysis of the boundary conditions for a Hele–Shaw bubble. Phys. Fluids A 2, 1105–1117.

Calvert, J.R., 1990. Pressure drop for foam flow through pipes. Int. J. Heat Fluid Flow 11, 236–241.

Calvert, J.R., Nezhati, K., 1986. A rheological model for a liquid–gas foam. Int. J. Heat Fluid Flow 7, 164–168.

Cognet, G., 1968. Contribution à l'étude de l'écoulement de Couette par la méthode polarographique, Thèse, Nancy.

Coney, M.W.E., 1973. The theory and application of conductance probes for the measurement of liquid film thickness in two-phase flow. J. Phys. E: Sci. Instrum. 6, 903–910.

Deslouis, C., Gil, O., Tribollet, B., 1990. Frequency response of electrochemical sensors to hydrodynamics fluctuations. J. Fluid Mech. 215, 85–100.

Enzendorfer, C., Harris, R.A., Valko, P., Economides, M.J., 1994. Pipe viscosimetry of foams. J. Rheol. 39, 345–358.

Funfschilling, P., 2001. Investigation par un écoulement de Couette de la réponse fréquentielle des sondes électrochimiques et de la floculation de particules en suspension, Thèse, Nancy.

Gardiner, B.S., Dlugogorski, B.Z., Jameson, G.J., 1999. Prediction of pressure losses in pipe flow of aqueous foams. Ind. Eng. Chem. Res. 38, 1099–1106.

Harris, W., Radke, C.J., Morris, S., 1994. The motion of long bubbles in polygonal capillaries. J. Fluid Mech. 292, 71–110.

Kraynick, A.M., 1988. Foam flows. Annu. Rev. Fluid Mech. 20, 325–357.

Kroezen, A.B.J., Groot, W.J., Schipper, C.A.C., 1988. The flow properties of foam. JSDC 108, 393–400.

Lebouché, M., 1968. Contribution à l'étude des mouvements turbulents des liquides par la méthode polarographique, Thèse, Nancy.

Levêque, M.A., 1928. Les lois de la transmission de la chaleur par convection. Ann. Mines Carbur. 13, 201–239.

Lusseyran, F., 1990. Caractéristiques cellulaires du régime à poches en écoulement gaz-liquide co-courant vertical. Transition vers le régime déstructuré, Thèse, Nancy.

Mao, Z., Hanratty, T.J., 1991. Analysis of wall shear stress probes in large amplitude unsteady flows. Int. J. Mass Transfer 34, 281–290.

Mitchell, J.E., Hanratty, T.J., 1966. A study of turbulence at a wall using an electrochemical wall shear stress meter. J. Fluid Mech. 26, 199–221.

Nakoryakov, V.E., Burdukov, A.P., Kashinsky, O.N., Geshev, P.I., 1986. Electrodiffusion method of investigation into local structure of turbulent flows. Thermophysics Institute Novosibirsk, p. 247.

Prud'homme, R.K., Khan, S.A., 1996. Experimental results on foam rheology. Surfactant Sci. Ser. 57, 217–241.

Ratulowski, J., Chang, H., 1989. Transport of gas bubbles in capillaries. Phys. Fluids A 1, 1642–1655.

Reiss, L.P., Hanratty, T.J., 1963. An experimental study of the viscous sublayer. AIChE J. 2, 154–160.

Sobolik, V., Wein, O., Wichterle, K., 1996. Transient technique in electrodiffusion measurements. In: Proc. of 4th Electro. Diffusion Workshop, Lahnstein.

Souhar, M., 1982. Contribution àl'étude dynamique des écoulements diphasiques gaz-liquide en conduite verticale: cas des régimes àbulles et àpoches. Thèse, Nancy.

Thondavadi, N.N., Lemlich, R., 1985. Flow properties of foam with and without solid particles. Ind. Eng. Chem. Process Des. Dev. 24, 748–753.

Wenzel, H.G., Brungraber, R.J., Stelson, T.E., 1970. The viscosity of high expansion foam in pipes. J. Mater. JMLSA 5, 396–412.

Yoshimura, A., Prud'homme, R.K., 1988. Wall slip corrections for Couette and parallel disk viscometers. J. Rheol. 32, 53–67.